The Annual and Semiannual Cycles of the Tropical Wind Field

DAVID S. GUTZLER*

Cooperative Institute for Research in Environmental Studies (CIRES), University of Colorado/NOAA, Boulder, CO 80309

11 November 1986 and 25 March 1987

ABSTRACT

The annual and semiannual harmonics of the wind field within 25° of the equator at six tropospheric pressure levels are described, based on data from a network of rawinsonde stations. The annual cycle in the zonal wind component is most prominent in the upper troposphere at subtropical latitudes, with maximum westerlies occurring late in each hemisphere's winter season. Significant amplitudes of the annual cycle in the meridional wind component are found to be confined to layers about 150 mb thick at the bottom and top of the troposphere. The semiannual cycle is significant only in the zonal wind component. At stations near the equator, the semiannual cycle in zonal wind has larger amplitude than the annual cycle.

1. Introduction

Harmonic analysis provides a concise, quantitative description of annual variability. Harmonics can be particularly illustrative climatic diagnostics in the tropics, where solar radiative forcing contains strong periodicities at both annual (12-month) and semiannual (6-month) frequencies (Stephens et al., 1981). Harmonic analysis of the annual variability of surface parameters in the tropics has been extensively carried out. The annual and semiannual cycles (or harmonics) of precipitation, sea level pressure, and surface temperature over the globe were presented by Hsu and Wallace (1976a,b), White and Wallace (1978), and Shea (1986). Horel (1982) calculated the annual and semiannual harmonics of surface wind, sea level pressure, sea surface temperature, and rainfall over the Pacific.

Much less documentation of the annual and semiannual harmonics at higher levels has been done. Arkin et al. (1986) used time series of the National Meteorological Center (NMC) operational tropical analysis to calculate the annual cycle of the 200 mb zonal and meridional wind components, rotational and divergent wind components, and outgoing longwave radiation. The semiannual cycle of the zonal wind and temperature fields in the tropical free atmosphere were calculated from rawinsonde station data by van Loon and Jenne (1969, 1970). The signal they described included semiannual westerly wind maxima at 200 mb in May and November throughout the tropics and the Southern Hemisphere. Phase reversals (easterly wind maxima in May and November) were observed above the equatorial tropopause and in the lower troposphere. Similar semiannual cycles were found in the temperature field of the near-equatorial troposphere (with May–November maxima) and subtropical Southern Hemisphere over Australia (with May–November minima), and in the latitude of the axis of the Southern Hemisphere subtropical jet stream (positioned furthest equatorward in May and November). These semiannual cycles were interpreted by van Loon and Jenne in terms of the north–south seasonal shift of the Hadley circulation, with maximum upper tropospheric westerlies and lower tropospheric easterlies in both hemispheres occurring when the outflow associated with latent heating originates on the equator, consistent with angular momentum conservation.

This paper presents a three-dimensional description of the annual and semiannual harmonics of tropical winds. Emphasis is placed on the vertical structures of each harmonic. In order to maximize data reliability, the statistics are calculated from station data rather than an analysis product. The horizontal resolution of the network of available rawinsonde stations is extremely coarse, but still significantly larger than the station sample used by van Loon and Jenne (1969, 1970).

Two issues of relevance to large-scale air–sea interaction studies will be addressed. One is a comparison of the annual and semiannual harmonics of the 850 mb wind field (the lowest level included in this dataset) with previous studies of the harmonics of surface variables. The surface wind field is a crucial boundary condition for ocean circulation variability on seasonal time scales, but the meteorological community often uses the 850 mb wind field to describe the low-level atmospheric circulation over the oceans. A limited comparison of surface and 850 mb wind statistics was recently carried out by Harrison and Gutzler (1986), who calculated monthly wind climatologies for five western

* Current affiliation: Atmospheric and Environmental Research, Inc., Cambridge, MA 02139.

Pacific islands. Significant climatological wind shears were found, varying widely with location and to a lesser extent with season. Here we extend their comparison to the annual and semiannual harmonics of the wind field.

The role of the annual cycle in regulating the evolution of interannual signals such as the El Niño–Southern Oscillation (or ENSO) phenomenon is also a question of widespread interest. In the equatorial eastern Pacific, the sea surface temperature (SST) anomaly known as El Niño tends to amplify off the South American coast early in the year, when the SST reaches its climatological annual maximum as well (Rasmusson and Carpenter, 1982). The patch of warm water then typically shifts slowly westward with time, also in concert with the westward "propagation" of the SST annual cycle maximum (Horel, 1982). Recently Meehl (1987) has proposed that the evolution of Southern Oscillation "Warm Events" in the atmosphere over the western equatorial Pacific also represents an amplification of the annual cycle. He documented the climatological southeastward movement of the "convective maximum" across this region from the Indian subcontinent in July, to the Indonesian region in October, and onward to the New Guinea–North Australia region in January, and found that Warm Events often developed following yearly episodes during which the convective maximum moves eastward with the same phase but anomalously large amplitude. Gutzler and Harrison (1987) showed that the evolution of seasonal zonal wind anomalies over the western Pacific during the incipient stages of five of the six most recent El Niño/Southern Oscillation (ENSO) events was "phase-locked" to the calendar. In the Northern Hemisphere autumn season preceding El Niño, lower tropospheric near-equatorial zonal winds converges over the Indonesian region, overlain by upper tropospheric divergence. This pattern propagates eastward as the ENSO event develops. In this paper, we will consider whether the phase-locked eastward propagation of zonal wind anomalies described by Gutzler and Harrison (1987) could represent an amplification of the climatological variability of the zonal wind field over the tropical western Pacific.

The scope of this study is limited by the coarseness of the station network. Ultimately, the large gaps between rawinsonde stations can be filled by analysis products, and the dynamical mechanisms underlying the periodic variability can be diagnosed using climate models which simulate the annual and semiannual cycles. However, it is essential that analysis schemes and climate models represent observed data faithfully. The cycles documented in this paper should serve as benchmark statistics for analyses and models.

The steps taken to check the data and calculate the harmonics are described in section 2. The vertical structure and geographical distribution of the amplitude and phase of the annual and semiannual cycles are presented in section 3. In section 4, the results are summarized and some implications for climate studies and analysis schemes are discussed.

2. Data and analysis procedures

The monthly mean observations used in this study were obtained from *Monthly Climatic Data for the World,* archived on tape at the National Center for Atmospheric Research. Thirty-four stations were selected for study, each located within 25° of the equator and having a data record at least 7 yr long. A list of the stations and a summary of each station's record are given in Table 1. The abbreviated station names in the Table correspond to the map of station locations in Fig. 1. Data at six levels (850, 700, 500, 300, 200, and 150 mb) were considered. No surface winds are included in this dataset, and the average number of observations incorporated in the monthly means falls off rapidly with height above 150 mb. The data record extends through the end of 1980.

Data quality was checked carefully. First, duplicate records and records with one or more of the six levels of interest missing were removed from the time series. Then, the mean and variance at each level for each calendar month were computed. These statistics were used to calculate time series of monthly anomalies, and monthly anomalies normalized by the interannual standard deviation. The time series were examined for suspicious data, with special attention paid to observations departing from the calendar monthly mean by more than three standard deviations. A similar technique was employed by Trenberth and Paolino (1980) to identify suspicious values in time series of monthly mean sea level pressure.

Attempts were made to check suspicious data against two independent sources: the monthly averaged National Meteorological Center (NMC) Tropical Analysis of 200 mb winds for the period 1968–74 and an atlas of monthly averaged 200 mb and 850 mb streamfunction fields for the period 1965–74 (Krishnamurti et al., 1983). Contemporaneous reports from nearby stations were also considered in some cases.

A conservative approach to data rejection was maintained. Only values judged to be physically inconceivable were eliminated from the time series. In some cases, the source of error was obvious (e.g., units digit dropped from the reported wind direction) and corrected values substituted into the time series. Monthly mean records containing an apparently erroneous wind datum at any level, without a readily identifiable correction, were eliminated from the time series without substitution.

Monthly climatologies for each station and pressure level were then recalculated from the time series of monthly means. Because some gaps are present in the time series, the resulting monthly climatologies are based on different sets of years, but no attempt was made to adjust the climatologies to compensate for the

TABLE 1. Stations used and period of record for each wind time series. Station abbreviations refer to Fig. 1.

Station abbreviation	Name	Lat	Long	Period of record
ABI	Abidjan	5.3°N	3.9°W	Jan 1964–Oct. 1980
ANT	Antofagasta	23.5°S	70.4°W	Aug. 1957–Dec. 1980
ATU	Atuona	9.8°S	139.0°W	Apr. 1969–Jan. 1980
BAN	Bangkok	13.7°N	100.5°E	Jan. 1957–May 1980
BEL	Belem	1.4°S	48.5°W	Aug. 1968–June 1975
BOG	Bogota	4.6°N	74.1°W	Sept. 1960–Dec. 1979
CAL	Calcutta	22.5°N	88.4°E	Apr. 1964–Dec. 1980
CAN	Canton	2.8°S	171.7°W	Jan. 1957–Aug. 1967
COC	Cocos	12.1°S	96.9°E	July 1964–Nov. 1980
DAK	Dakar	14.7°N	17.5°W	Jan. 1964–Dec. 1980
DES	Dar es Salaam	6.9°S	39.2°E	June 1961–Dec. 1977
DAR	Darwin	12.4°S	130.9°E	July 1964–Nov. 1980
FLM	Fort Lamy	12.1°N	15.0°E	June 1964–Dec. 1978
HIL	Hilo	19.7°N	155.1°W	Jan. 1957–Dec. 1980
JOH	Johnston	17.0°N	169.5°W	Jan. 1959–Dec. 1980
KHA	Khartoum	15.6°N	32.6°E	Jan. 1964–Dec. 1980
KOR	Koror	7.3°N	134.5°E	Sept. 1957–Dec. 1980
KIN	Kota Kinabalu	6.0°N	116.1°E	Mar. 1968–Dec. 1980
LAE	Lae	6.7°S	147.0°E	Sept. 1964–July 1973
LIM	Lima	12.0°S	77.1°W	May 1967–Dec. 1980
MAJ	Majuro	7.1°N	171.4°E	Jan. 1959–Dec. 1980
MIA	Miami	25.8°N	80.3°W	Jan. 1957–Oct. 1977
NAI	Nairobi	1.3°S	36.8°E	Feb. 1958–Dec. 1980
NAT	Natal	5.9°S	35.3°W	Jan. 1968–Dec. 1980
NOU	Noumea	22.3°S	166.5°E	July 1964–Dec. 1980
PAG	Pago Pago	14.3°S	170.6°W	Apr. 1966–Dec. 1980
PSU	Port Sudan	19.6°N	37.2°E	Jan. 1964–Dec. 1975
SAN	San Andres	12.8°N	81.7°W	June 1957–Feb. 1980
SIN	Singapore	1.3°N	103.9°E	Mar. 1960–Dec. 1980
TAH	Tahiti	17.6°S	149.6°W	Jan. 1964–Dec. 1980
TRI	Trinidad	10.7°N	61.5°W	Aug. 1967–Dec. 1980
TRV	Trivandrum	8.5°N	77.0°E	Jan. 1963–Dec. 1980
TRU	Truk	7.5°N	151.9°E	Sept. 1957–Dec. 1980
VER	Veracruz	19.2°N	96.1°W	Feb. 1964–Dec. 1980

gaps. The annual and semiannual cycles (hereafter denoted M_1 and M_2, respectively) of the zonal and meridional wind components u and v were then defined at each station and pressure level as the Fourier harmonic with periods of 12 and 6 months, respectively, calculated from each monthly climatological time series.

The phases of the harmonics are referred to in terms of phase maxima—the time of year when the wind associated with a harmonic reaches its westerly or southerly maximum—and minima—easterly or northerly maximum. The harmonics are plotted in a vector format similar to that employed by Hsu and Wallace (1976a,b), White and Wallace (1978), Horel (1982), and Arkin et al. (1986). Vectors directed southward, westward, northward, and eastward correspond to phase maxima in mid-January, mid-April, mid-July, and mid-October, respectively.

3. Annual and semiannual cycles

a. Annual cycles of u and v

The magnitude of the annual cycle in the zonal wind at 850 mb (Fig. 2a) is greatest in the sector bounded

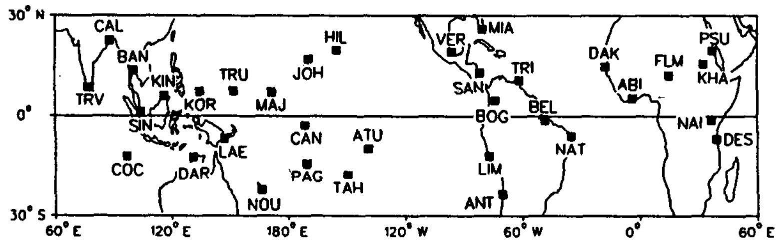

FIG. 1. Map of station locations. (See Table 1 for key to abbreviations.)

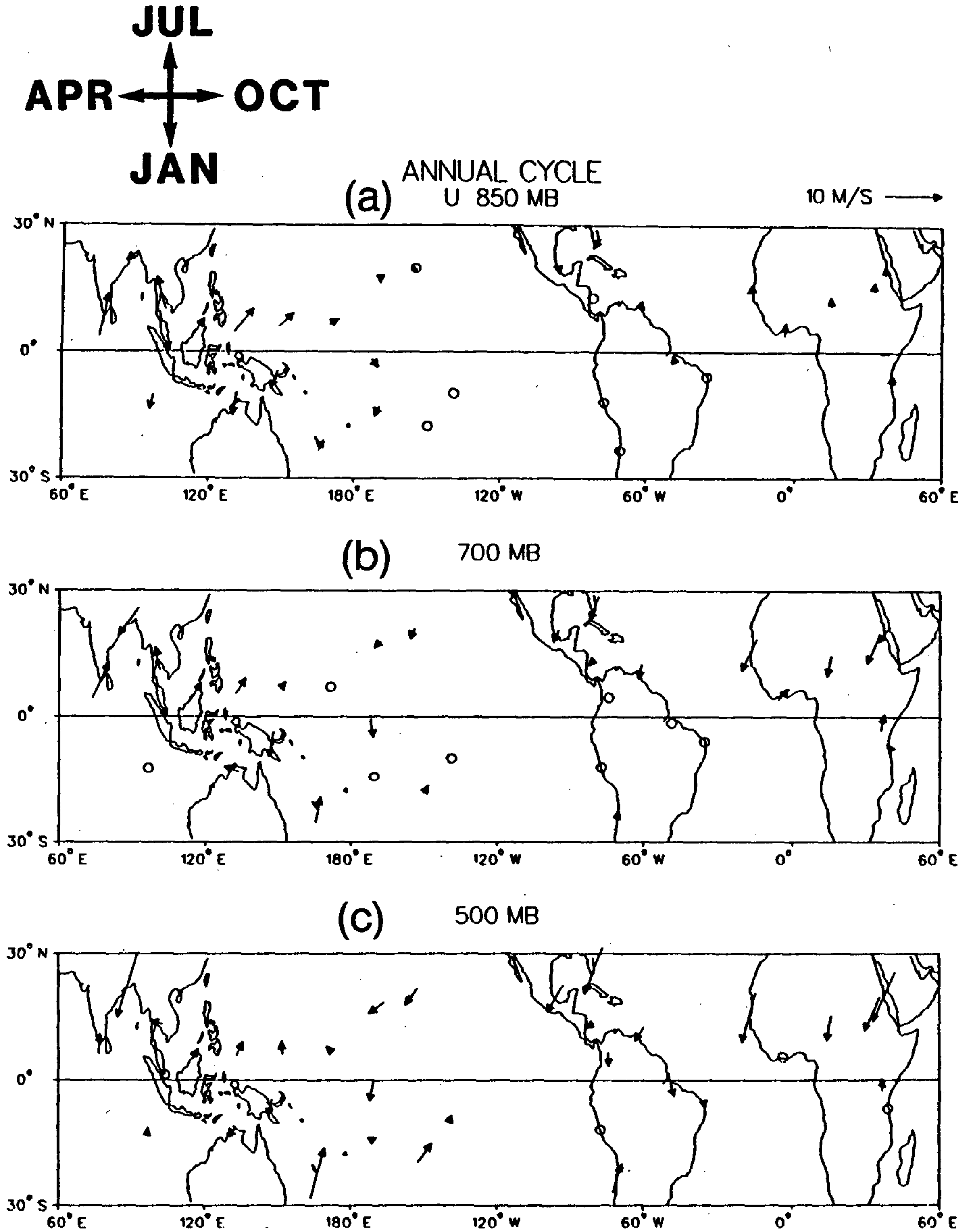

FIG. 2. Vector plots of the annual cycle of the zonal wind component. The length of each vector is proportional to the amplitude of the annual (12-month) harmonic, with scale vector in the upper right corner of each set of three plots. Vectors are centered on the station locations. The orientation of each vector represents the phase of the harmonic: southward-directed vectors signify phase maxima (times of maximum westerlies) in mid-January, with the phase progressing clockwise, so that westward-directed vectors signify phase maxima in mid-April, and so forth. Zero is plotted at stations where the amplitude of the annual cycle is less than 1 m/s. (a) 850 mb, (b) 700 mb, (c) 500 mb, (d) 300 mb, (e) 200 mb and (f) 150 mb.

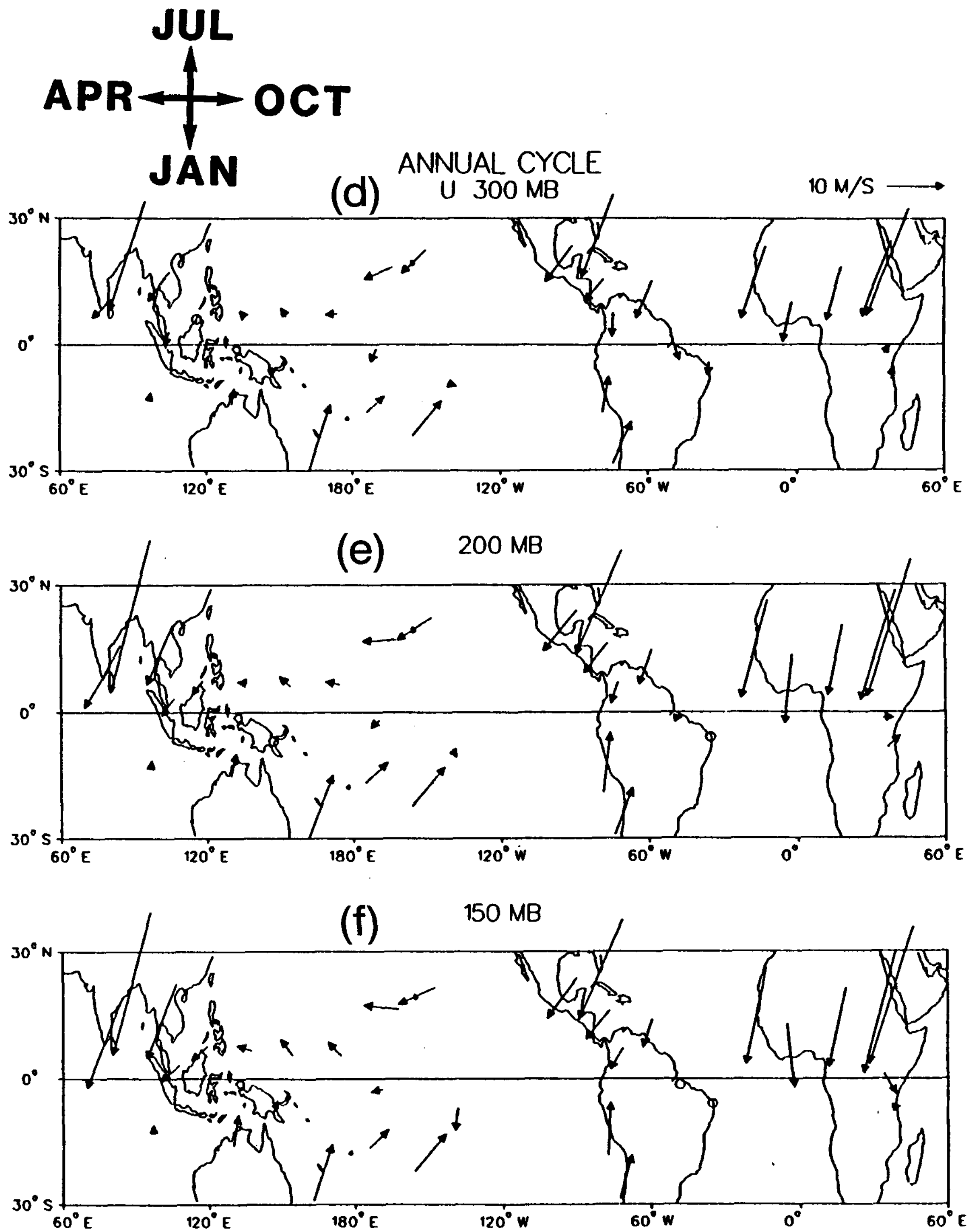

FIG. 2. (*Continued*)

by 5°–15°N and 60°–140°E, where the amplitude exceeds 5 m/s, with phase maxima during the northern summer. Moving eastward into the mid-Pacific, the magnitude of $M_1(u)$ decreases and its phase maximum shifts from early July at Bangkok to early October at Majuro. The local phases of $M_1(u)$ over the Pacific agree closely with the phases of the annual harmonic of the surface zonal wind field (Horel, 1982) and outgoing longwave radiation (Arkin et al., 1986). Because the speed of the annual mean 850 mb wind increases from

Southeast Asia eastward over the mid-Pacific (not shown) where $|M_1(u)|$ decreases eastward, the western tropical Pacific is a transition zone between a monsoonal regime in the lower tropospheric circulation near the Asian continent, and a steady trade regime over the central Pacific. South of the equator between about 60°E and 160°W, the phase of $M_1(u)$ is reversed compared to the Northern Hemisphere stations, with phase maxima in late southern summer. $M_1(u)$ has very small amplitude at stations within 2° latitude of the equator and at Southern Hemisphere stations located from 160°W eastward to 100°E.

At all stations poleward of 15° in both hemispheres, the amplitude of $M_1(u)$ increases monotonically with height up to 200 mb. Phase maxima occur late in the local winter, except over the subtropical central Pacific, where phase maxima in the upper troposphere occur during early to midspring (as at Tahiti and Johnston, for example). Weak springtime phase maxima at 200 mb are observed at near-equatorial Pacific stations north of the equator. Equatorward of 15°, amplitudes either decrease with height in the lower troposphere (e.g., Trivandrum and Darwin), or remain small from 850 mb up to the 500 mb level (e.g., Singapore and Lima). The amplitude increases sharply above 300 mb everywhere except at a few stations very close to the equator (e.g., Canton and Belem), where the annual variability of the upper tropospheric zonal wind field is contained primarily in the semiannual cycle.

The annual cycle in the meridional wind component $M_1(v)$ for each level is plotted in Fig. 3. At 850 mb, the amplitude of $M_1(v)$ is greater than the amplitude of $M_1(u)$ at a few stations over continents or along coastlines. Examples are Dar es Salaam on the east coast of Africa, where a strong low level southerly jet occurs from May through September, and Singapore and Calcutta, where monsoon circulations dominate the annual harmonic. At all stations in the tropical central and western Pacific, $M_1(v)$ is small (on the order of 1 m/s). The phase of $M_1(v)$ near the equator is nearly constant at all longitudes (phase maxima in July), corresponding to the seasonal alternation in the strength of the Hadley circulation, with low-level cross-equatorial flow directed into the summer hemisphere.

The amplitude of $M_1(v)$ decays rapidly with height in the lower troposphere: at the surface, $|M_1(v)| > |M_1(u)|$ throughout the Pacific (Horel, 1982). At 850 mb, the inequality is reversed over the Pacific (Fig. 3a; see also Harrison and Gutzler, 1986). Phase reversals in $M_1(v)$ are evident poleward of the trade wind maximum at 850 mb at Hilo and at 700 mb at Antofagasta, but the reversals are very much weaker than the corresponding reversal in the surface wind field shown by Horel (1982). At 500 mb (Fig. 3c), $M_1(v)$ is negligible.

At 300 mb and above, $|M_1(v)|$ increases rapidly with height, with a February maximum over the western Pacific and Southeast Asia, and similar phase but smaller amplitude south of the equator. Amplitudes are also small over the central near-equatorial Pacific, with a phase shift of about 3 months (phase maxima in late April) relative to stations farther west.

b. Semiannual cycle of u

Plots of the amplitude and phase of the semiannual cycle of the zonal wind $M_2(u)$ are shown in Fig. 4. The plotting convention is the same as for the annual cycle plots, with arrowheads on both ends of each vector to signify the double maximum associated with the semiannual cycle. The amplitude of the semiannual cycle of the meridional wind field $M_2(v)$ is less than 2.5 m/s at all stations and pressure levels and typically less than 1 m/s, so plots of $M_2(v)$ are not shown.

At stations between longitudes 0° and 120°E, the semiannual signal in u in these data is consistent with the description of van Loon and Jenne (1969, 1970). In the upper troposphere, phase maxima occur in May and November, with amplitudes between 4 and 5 m/s at 200 mb. The phase reverses near 500 mb, below which phase maxima occur in January and July with amplitudes between 1.5 and 3 m/s.

The $M_2(u)$ exhibits several different structures in other regions. Over the western near-equatorial Pacific, the upper tropospheric signal is the same as at stations farther to the west, but no midtroposphere node occurs. Instead, the phase of $M_2(u)$ shifts gradually to earlier phase maxima with decreasing height, with phase maxima in March–September at 850 mb. The longitudinal phase shift of $M_2(u)$ at 850 mb near 120°E just north of the equator (between Bangkok and Koror) suggests the presence of a semiannual cycle of zonal wind convergence, with the low-level zonal wind field associated with M_2 converging near 120°E in May–November and diverging in February–August. No discernible counterpart to this feature is observed in the upper troposphere, but such low-level convergence is consistent with the May–November semiannual precipitation maxima at stations on Borneo found by Hsu and Wallace (1976a). At subtropical latitudes in both hemispheres from the central Pacific eastward across the Americas, $M_2(u)$ in the upper troposphere again has May–November phase maxima, but has almost zero amplitude in the lower troposphere.

Stations within about 12° latitude of the equator between about 180° and 30°W longitude (delineated in the 200 mb plot by the dashed box in Fig. 4e, with similar geographical structure evident at 150 mb in Fig. 4f) exhibit a much weaker semiannual cycle, with some suggestion of a phase reversal compared to the region between 0°–120°E. The longitudinal phase reversal of $M_2(u)$ would imply a semiannual tendency for lower tropospheric convergence (divergence) and upper tropospheric divergence (convergence) in May–November at 30°W (180°), and the reverse tendency in February–August.

More detailed documentation of this circulation cell is hampered by the absence of stations over the eastern Pacific, but considerable corroborative evidence consistent with this result can be found in other studies. The data of van Loon and Jenne (1969) included a phase reversal of $M_2(u)$ at 200 mb at Recife [8°S 35°W] relative to $M_2(u)$ at 200 mb at the seven other near-equatorial stations they examined. Hsu and Wallace (1976a) show that January–July semiannual precipitation maxima occur at equatorial Pacific islands near the date line. Weickmann and Chervin (1987) find a semiannually varying circulation cell with this structure in a study of the climatological variability of 250 and 850 mb analyzed wind fields.

Hsu and Wallace (1976a) and White and Wallace (1978) have pointed out that the semiannual cycle, though mathematically distinct, may represent merely a modulation of the annual cycle when the amplitude of M_1 is much greater than M_2 or when the variable in question is nonnormally distributed (such as precipitation, which cannot be negative). The phase of $M_2(u)$ in the upper troposphere is typically in quadrature with $M_1(u)$, indicative of broad winter minima and sharp summer maxima in both hemispheres. However, the amplitude of $M_2(u)$ is geographically uniform over much of the tropical eastern hemisphere, even in regions where $M_1(u)$ is small, suggesting that $M_2(u)$ is appropriately interpreted as a separate "mode" of zonal wind variability, and not just as a modulation of $M_1(u)$.

c. *Reproducibility of annual and semiannual harmonics*

The annual mean and annual and semiannual cycles were calculated for separate decades 1961–70 and 1971–80 at all stations whose data records were sufficiently long (not shown). For all harmonics with amplitudes greater than 1 m/s, the amplitudes derived from separate decades were reproducible to within 15%, and phases agreed to within 1 month. In addition to confirming the reliability of the harmonic statistics, the reproducibility of the harmonics indicates the lack of any recent significant trends in the annual cycle on decadal time scales. Furthermore, the consistency between decades indicates that the presence of a peak in tropical wind variance spectra at a period of 40–50 days (Madden and Julian, 1971) does not significantly alias the calculation of *climatological* monthly mean winds.

4. Discussion

Over the near-equatorial western Pacific, the phase of $M_1(u)$ in the lower and upper troposphere and $M_1(v)$ in the upper troposphere shifts by about 3 months between Bangkok and Majuro, as shown in Figs. 2 and 3. While this phase shift toward later phase maxima over the central Pacific may bear some resemblance to the eastward movement of the convective maximum described by Meehl (1987), it is not so clear that one could describe the ENSO-associated wind anomaly pattern shown by Gutzler and Harrison (1987) as an amplification of the annual harmonic of the zonal wind field. The three-dimensional climatological signal in u over the western Pacific is complicated, because both the annual harmonic $M_1(u)$ and the semiannual harmonic $M_2(u)$ have significant amplitudes but different vertical structures. The relationship between the wind field and convection (both for climatological and interannual variability) remains an important topic for future research.

Within 10° of the equator, the climatological meridional wind field has significant amplitude only within layers approximately 150 mb thick at the top and bottom of the troposphere. The meridional winds at any particular latitude generally vary in phase throughout the tropics, and out of phase between the bottom and top of the troposphere.

Throughout the western and central tropical Pacific, the magnitude of $M_1(v)$ is much smaller at 850 mb compared with the surface wind field, suggesting that the effects of surface temperature gradients, which dominate the annual variability of the surface wind circulation over the eastern Pacific (Horel, 1982; Nigam and Lindzen, 1987) are significantly damped by the 850 mb level. As pointed out previously by Harrison and Gutzler (1986), it is extremely difficult to extrapolate low-frequency meridional wind variations from the 850 mb level to the surface.

The meridional wind variability described by $M_1(v)$ is consistent with the seasonal variations evident in the analyses of Newell et al. (1972) and Oort (1983), which were also based directly on station data, verifying that the annual harmonic is the dominant component of the seasonal variability of the meridional wind. However, the largest amplitudes of $M_1(v)$ at 200 mb shown in Fig. 3e (along the west coast of the Americas, and north of the equator over the Indonesian region) are 25–50% larger than the analysis-derived harmonics calculated by Arkin et al. (1986) (based on analyses from the period subsequent to September 1978, when NMC switched away from a nondivergent analysis scheme; McPherson et al., 1979). The meridional wind field at 200 mb in the operational analysis still appears to be deficient, despite the incorporation of divergent circulation modes into the analysis. The agreement between $M_1(v)$ at 200 mb in the station data and $M_1(v)$ in the NMC analysis is better over regions where $|M_1(v)|$ is smaller.

The narrow width of the upper tropospheric layer of strong meridional wind may be a source of problems in the analysis scheme. Rosen and Salstein (1985) compared pre- and postinitialized NMC analyses with station observations for 2 separate months (January

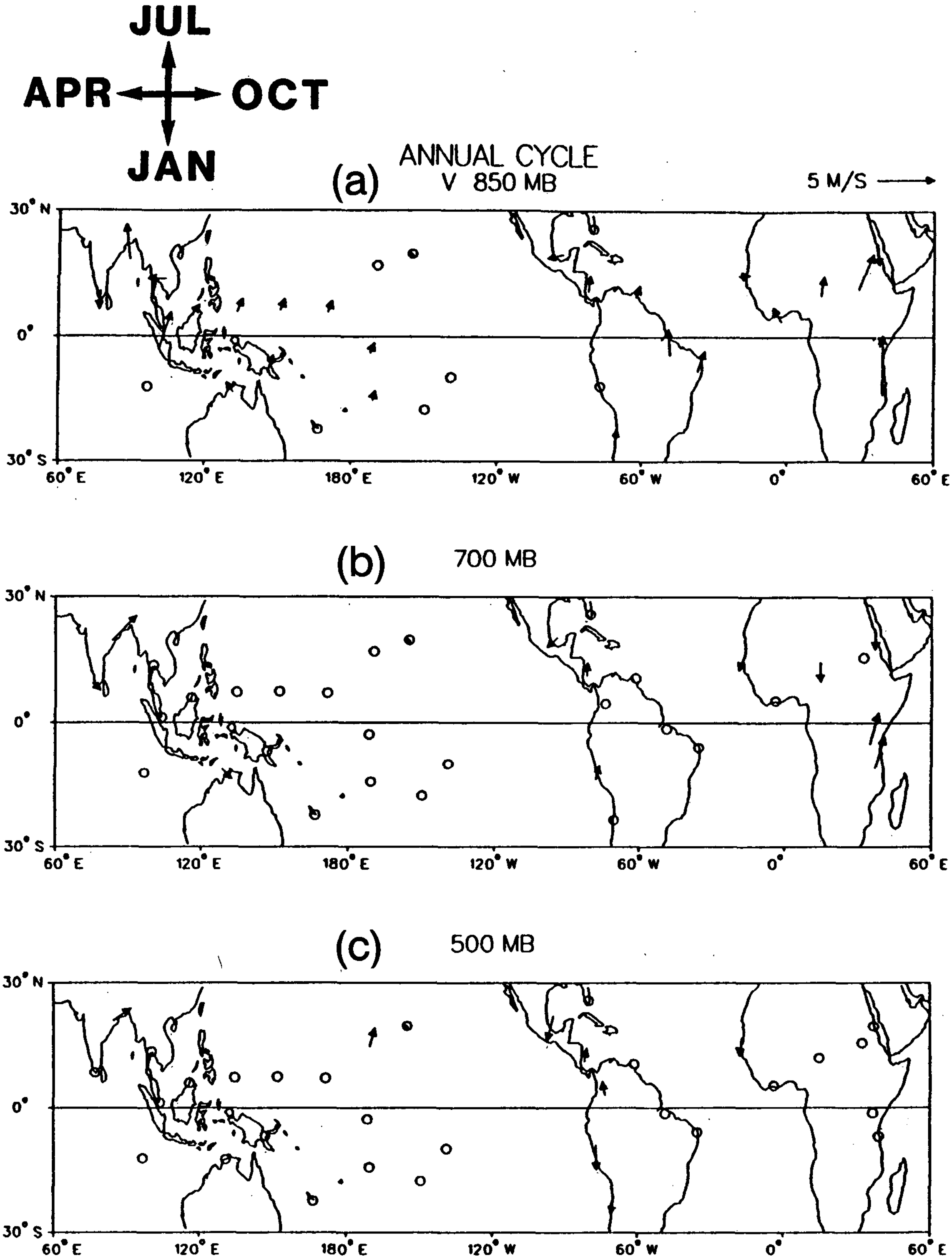

FIG. 3. As in Fig. 2, but for the annual cycle of the meridional wind component. Note that the scale is doubled relative to Fig. 2. Phase maxima represent times of maximum southerlies.

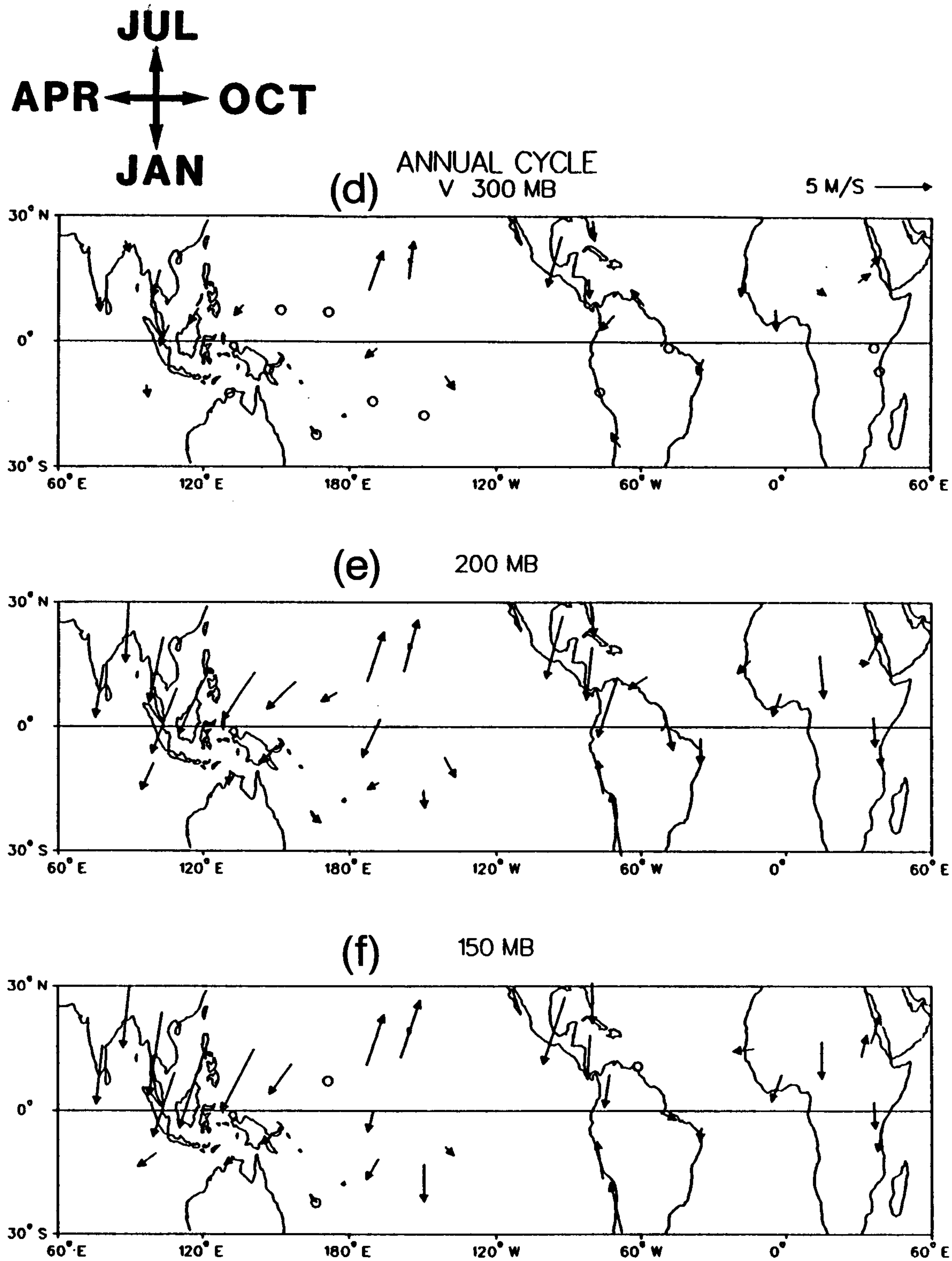

FIG. 3. (*Continued*)

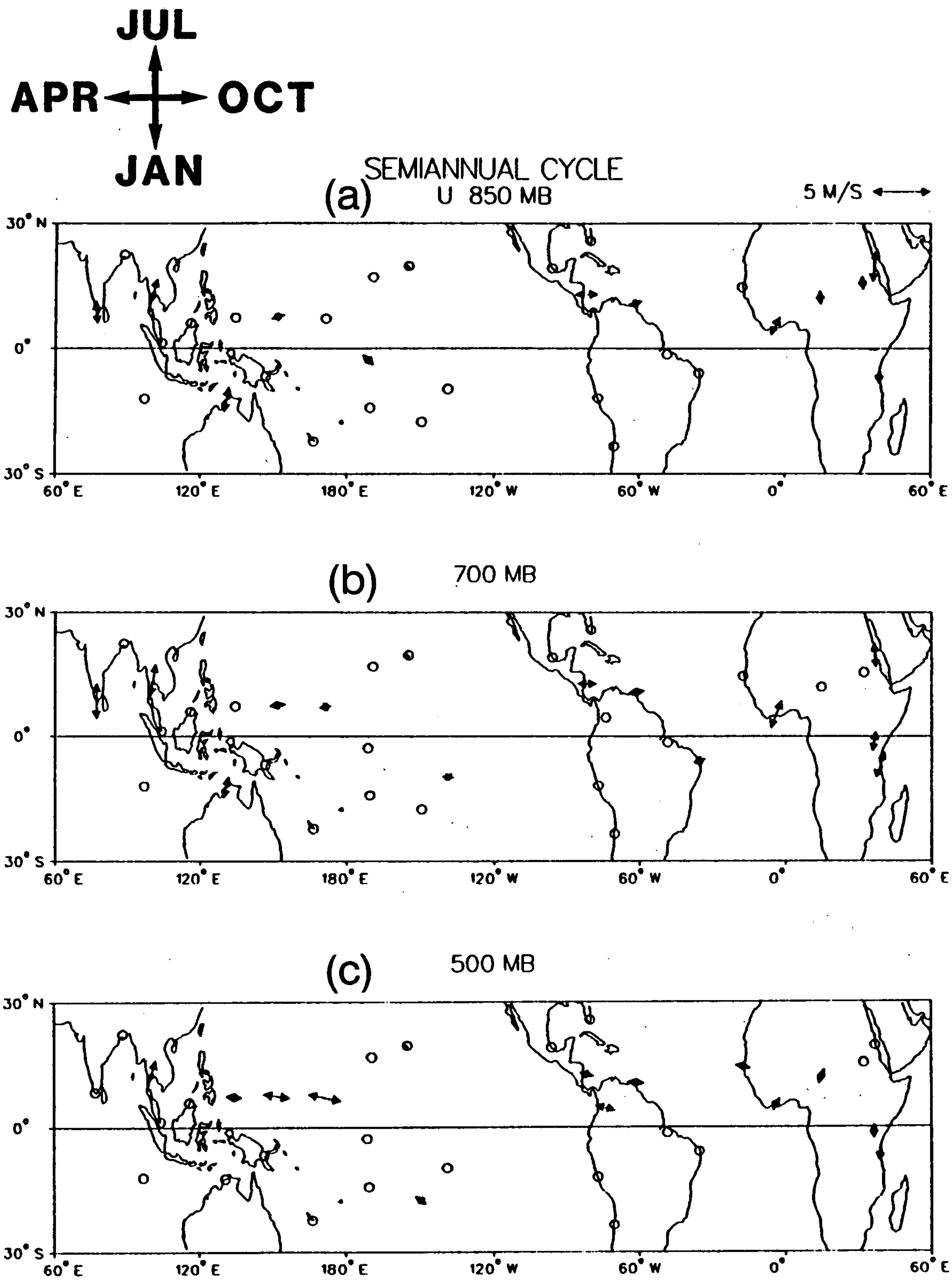

FIG. 4. As in Fig. 2, but for the semiannual cycle (6-month harmonic) of the zonal wind component. Note the double arrowheads on each vector, indicating the twice-yearly phase maxima associated with the semiannual cycle. [See text for explanation of dashed box in (e).]

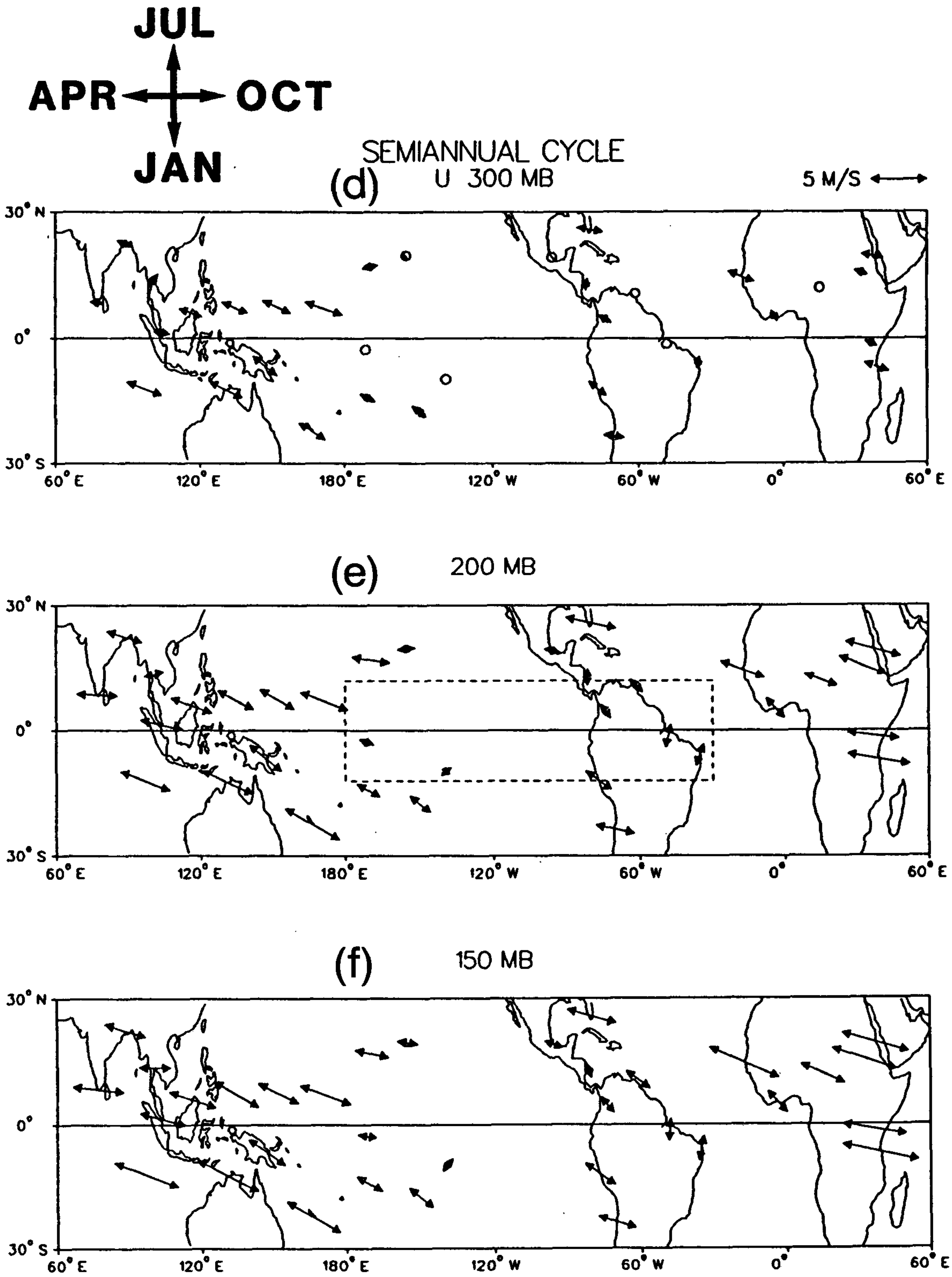

FIG. 4. (*Continued*)

and July 1983), and concluded that the magnitude of the total mean meridional mass transport was not strongly modified by the initialization process. However, their calculation of the mean meridional circulation (their Fig. 1) suggests that the initialization process significantly smooths the vertical gradients of the divergent meridional flow in the upper troposphere. Therefore, even if the total meridional mass transport is correct in the resulting analysis, the initialization scheme could produce divergent meridional winds that are too weak at the levels of maximum wind by distributing the mass transport over a pressure layer that is too thick. Analyses of the tropical upper tropospheric circulation for the FGGE year indicate that divergent and rotational components of v are of comparable magnitude (Paegle et al., 1983), so vertical smoothing of the divergent wind could contribute significantly to the reduction in amplitude of $M_1(v)$ at 200 mb in the Arkin et al. (1986) analysis-based calculation compared to the results shown here.

REFERENCES

Arkin, P. A., V. E. Kousky, J. E. Janowiak and E. A. O'Lenic, 1986: Atlas of the tropical and subtropical circulation derived from National Meteorological Center operational analyses. NOAA Atlas No. 7, 59 pp. [available from Climate Analysis Center, W/NMC52, Washington, DC 20233]

Gutzler, D. S., and D. E. Harrison, 1987: The structure and evolution of seasonal wind anomalies over the near-equatorial eastern Indian and western Pacific Oceans. *Mon. Wea. Rev.,* **115,** 169–192.

Harrison, D. E., and D. S. Gutzler, 1986: Variability of monthly-averaged surface and 850 mb winds at tropical Pacific islands. *Mon. Wea. Rev.,* **114,** 285–294.

Horel, J. D., 1982: On the annual cycle of the tropical Pacific atmosphere and ocean. *Mon. Wea. Rev.,* **110,** 1863–1878.

Hsu, C.-P., and J. M. Wallace, 1976a: The global distribution of the annual and semiannual cycles in precipitation. *Mon. Wea. Rev.,* **104,** 1093–1103.

——, and ——, 1976b: The global distribution of the annual and semiannual cycles in sea-level pressure. *Mon. Wea. Rev.,* **104,** 1597–1601.

Krishnamurti, T. N., H.-L. Pan, R. Pasch and D. Subrahmanyam, 1983: *Interannual Variability of the Tropical Motion Field (Long-term Annual Cycle and Southern Oscillation).* FSU Report No. 83-3, Department of Meteorology, Florida State University, Tallahassee, FL 32306.

Madden, R. A., and P. R. Julian, 1971: Detection of a 40–50 day oscillation in the zonal wind in the tropical Pacific. *J. Atmos. Sci.,* **29,** 702–708.

McPherson, R. D., K. H. Bergman, R. E. Kistler, G. E. Rasch and D. S. Gordon, 1979: The NMC Operational global data assimilation system. *Mon. Wea. Rev.,* **107,** 1445–1461.

Meehl, G. A., 1987: The annual cycle and interannual variability in the tropical Pacific and Indian oceans. *Mon. Wea. Rev.,* **115,** 27–50.

Newell, R. E., J. W. Kidson, D. G. Vincent and G. J. Boer, 1972: *The General Circulation of the Tropical Atmosphere and Interactions with Extratropical Latitudes,* Vol. 1. The MIT Press, 258 pp.

Nigam, S., and R. S. Lindzen, 1987: On the role of sea surface temperature gradients in forcing low level winds and convergence in the tropics. *J. Atmos. Sci.,* **45,** accepted for publication.

Oort, A. H., 1983: Global Atmospheric Circulation Statistics, 1958–1973. NOAA Prof. Pap. 14, 180 pp. [NTIS PB8-4-129717]

Paegle, J., J. N. Paegle and F. P. Lewis, 1983: Large-scale motion of the tropics in observations and theory. *Pure Appl. Geophys.,* **121,** 947–982.

Rasmusson, E. M., and T. H. Carpenter, 1982: Variations in tropical sea surface temperature and surface wind fields associated with the Southern Oscillation/El Niño. *Mon. Wea. Rev.,* **110,** 354–384.

Rosen, R. D., and D. A. Salstein, 1985: Effect of initialization on diagnoses of NMC large-scale circulation statistics. *Mon. Wea. Rev.,* **113,** 1321–1337.

Shea, D. J., 1986: Climatological Atlas: 1950–1979. NCAR Technical Note NCAR/TN-269+STR, 35 pp. + figures. [available from Publications Office, NCAR, P.O. Box 3000, Boulder, CO 80307]

Stephens, G. L., G. G. Campbell and T. H. Vonder Haar, 1981: Earth radiation budgets. *J. Geophys. Res.,* **86,** 9739–9760.

Trenberth, K. E., and D. A. Paolino, 1980: The Northern Hemisphere sea-level pressure data set: Trends, errors and discontinuities. *Mon. Wea. Rev.,* **108,** 855–872.

van Loon, H., and R. L. Jenne, 1969: The half-yearly oscillations in the tropics of the Southern Hemisphere. *J. Atmos. Sci.,* **26,** 218–232.

——, and ——, 1970: On the half-yearly oscillations in the tropics. *Tellus,* **22,** 391–398.

Weickmann, K. M., and R. M. Chervin, 1987: The observed and simulated atmospheric seasonal cycle: I. Global wind field modes. Submitted to *Mon. Wea. Rev.*

White, G. H., and J. M. Wallace, 1978: The global distribution of the annual and semiannual cycles in surface temperature. *Mon. Wea. Rev.,* **106,** 901–906.